

# Gain Scheduled Automatic Flight Control Systems Design for a Light Commercial Helicopter Model

Erkan ABDULHAMITBILAL and Elbrous M. JAFAROV

Faculty of Aeronautics and Astronautics

Istanbul Technical University

Turkey

abdulhamitbilal@gmail.com, cafer@itu.edu.tr

*Abstract:* - In this paper, nonlinear rigid body dynamics for rotorcraft mathematical model is studied. A linearization of helicopter flight dynamics is evaluated. Automatic Flight Control System (AFCS) with gain scheduled LQ optimal control is designed based on look-up tables. Stability analyses are performed and results are illustrated graphically for open and closed-loop systems. As seen from results, LQ optimal control system pushes eigenvalues to left side of imaginary axis without excessive control inputs to maintain stability of naturally unstable rotorcraft dynamics. Proposed AFCS is tested by nonlinear flight dynamics model in Matlab-Simulink environment. Simulation results illustrate effectiveness of evaluated method and techniques.

*Key-Words:* - helicopter, flight dynamics, nonlinear model, simulation,

## 1 Introduction

Automatic Flight Control Systems (AFCSs) are electro-hydro mechanical systems that provide inputs to the control surfaces or elements to assist the pilot in maneuvering and handling the aircraft in desired flight conditions. The AFCSs provide both oscillation damping (dynamic stability) and maintain desired flight attitude, speed and heading (static stability). Major components of the AFCSs are stick, collective and pedals position sensors, servo accelerometers, flight control panel, flight computer, rate gyros, air data and speed transducers, etc.

In control theory, gain scheduling is an approach to control of non-linear systems that uses a set of linear controllers, which provides satisfactory control for a different operating point of the system. Scheduling variables are used to determine the operating region of the system and to enable the appropriate linear controller. In aircrafts, AFCSs have altitude and Mach number (or forward speed) as scheduling variables with different linear controller parameters available as look-up tables for various combinations of those two variables.

A full nonlinear mathematical model of helicopter dynamics of prototyped helicopter with trim, performance and linearization analyses, human pilot analysis, and AFCS design is studied in [1]. Design handbook of the flexible rotor used in the prototype

helicopter is given in [2]. Similarly full nonlinear rotorcraft dynamics model of Sikorsky UH-60A is studied in [3]. On the other hand, gain scheduled control system for the modeled prototype helicopter is evaluated in [4]. Similarly reconfigurable control for a tandem helicopter is investigated in [5]. Automatic flight control systems and flight dynamic are studied in [6-7]. Optimal control theory is evaluated in [8]. Gain scheduling theory and applications are studied in [9]. Helicopter flight dynamics and theory is researched in [10-12]. Some rotorcraft control systems such as state feedback and robust control are designed in [13-16]. Fuzzy and classical control approaches are applied to the problem in [17-18]. The significance of this paper is evaluation of the problem from beginning to the end which means modeling the rotorcraft dynamics, calculation of corresponding stability and control derivatives, design of control system for a flight envelope and simulation of control system with nonlinear flight dynamics.

In this paper, we will first study nonlinear rotorcraft equation of motion. Rotor dynamics and aerodynamics is not evaluated, but referred from [1] because these are hard to study in this paper. Then, we will linearize rotorcraft flight dynamics near a trim condition and propose a gain scheduled LQ optimal control law to be integrated in AFCS. We are going to perform all simulations with Matlab-Simulink on nonlinear flight dynamics model given at the end of the paper.

## 2 Problem Formulation

In this paper, we have considered a prototype helicopter designed and manufactured by Rotorcraft Design and Excellence Centre (ROTAM) - Istanbul Technical University (ITU) [1]. The rotorcraft has four flexible blades with Hanson’s rotor hub model [2]. Tail rotor is designed as conventional one and empennages are fixed. The helicopter is equipped with a turbo-shaft engine which produces 650 SHP (shaft horsepower). A picture of the rotorcraft from manufacturing phase is given in Figure 1 and some parameters for mathematical model are illustrated in Table 1.

Table 1 Some helicopter parameters [1]

<b>Main Rotor</b>	
Blade number.....	4 -
Radius.....	5.5 m
Rotor angular velocity.....	318 rpm
Blade twist.....	-10 deg
Rotor solidity.....	0.065 -
STA.....	5.0 m
BL.....	0.0 m
WL.....	5.7 m
<b>Tail Rotor</b>	
Blade number.....	2 -
Radius.....	0.914 m
Rotor angular velocity.....	2226 rpm
Rotor solidity.....	0.127 -
STA.....	11.6 m
BL.....	-0.4 m
WL.....	4.20 m
<b>Vertical Fin</b>	
Area.....	0.796 m <sup>2</sup>
Incidence.....	7.10 deg
STA.....	11.76 m
BL.....	0.17 m
WL.....	1.00 m
<b>Horizontal Stabilizer</b>	
Area.....	0.544 m <sup>2</sup>
Incidence.....	0.00 deg
STA.....	9.77 m
BL.....	0.40 m
WL.....	3.80 m
<b>Fuselage</b>	
Gross Weigh.....	2027 kg
STA.....	4.93 m
BL.....	0.01 m
WL.....	3.20 m



Figure 1 Prototyped Helicopter

Automatic Flight Control System (AFCS) proposed with this study consists of speed hold, height hold, and heading hold properties. Schematic view of AFCS panel on the board is shown in Figure 2. The panel includes a master switch to turn on/off the system. Speed, height and heading hold switches as well have on and off options. When the master switch is engaged, AFCS supplies short-term attitude and attitude rate stabilization to assist the pilot. For use in hands-free flight pilot must switched on speed hold, height hold, and heading hold switches. The rotorcraft will keep current flying speed just after turning speed hold switch on. Beside, height hold switch should be turned on to hold current flight altitude. If speed hold is on when height hold is turned on then control algorithm that runs for speed hold is cancelled and a new control law is replaced both for speed an altitude hold mode. And finally, turning heading switch on will keep rotorcraft heading angle at current flying yaw angle.

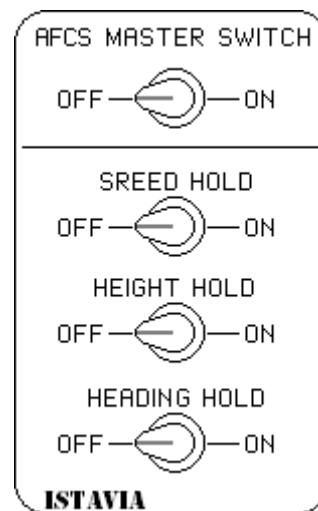


Figure 2 Schematic view of flight control panel

We should first define nonlinear flight dynamics of the rotorcraft to design a control law for

stabilization. Then we can easily linearize nonlinear dynamics near any trim point. Hence a LQ optimal control law, as we desire, can be structured.

The rigid-body equation of motion of the rotorcraft is as [1,3,6,11]:

$$\begin{bmatrix} \dot{u}_B \\ \dot{v}_B \\ \dot{w}_B \end{bmatrix} = \frac{1}{m} \begin{bmatrix} X \\ Y \\ Z \end{bmatrix} + g \begin{bmatrix} -s\theta_B \\ c\theta_B s\phi_B \\ c\theta_B c\phi_B \end{bmatrix} - \begin{bmatrix} 0 & -r_B & q_B \\ r_B & 0 & -p_B \\ -q_B & p_B & 0 \end{bmatrix} \begin{bmatrix} u_B \\ v_B \\ w_B \end{bmatrix} \quad (1)$$

$$\begin{bmatrix} \dot{p}_B \\ \dot{q}_B \\ \dot{r}_B \end{bmatrix} = I^{-1} \begin{bmatrix} L \\ M \\ N \end{bmatrix} - I^{-1} \begin{bmatrix} 0 & -r_B & q_B \\ r_B & 0 & -p_B \\ -q_B & p_B & 0 \end{bmatrix} I \begin{bmatrix} p_B \\ q_B \\ r_B \end{bmatrix} \quad (2)$$

$$\begin{bmatrix} \dot{\phi}_B \\ \dot{\theta}_B \\ \dot{\psi}_B \end{bmatrix} = \begin{bmatrix} 1 & s\phi_B t\theta_B & c\phi_B t\theta_B \\ 0 & c\phi_B & -s\phi_B \\ 0 & s\phi_B sc\theta_B & c\phi_B sc\theta_B \end{bmatrix} \begin{bmatrix} p_B \\ q_B \\ r_B \end{bmatrix} \quad (3)$$

where  $X, Y, Z$  are the acting total forces in (N);  $L, M, N$  are the acting total moments in (Nm);  $u_B, v_B, w_B$  are the body velocities in (m/s);  $p_B, q_B, r_B$  are the body angular rates in (rad/s);  $\theta_B, \phi_B, \psi_B$  are the body attitude angles in (rad);  $c = \cos, s = \sin, t = \tan, sc = \sec$ ;  $m$  is the mass in (kg) and  $I$  is the inertia matrix as:

$$I = \begin{bmatrix} I_{xx} & -I_{xy} & -I_{xz} \\ -I_{xy} & I_{yy} & -I_{yz} \\ -I_{xz} & -I_{yz} & I_{zz} \end{bmatrix} \quad (4)$$

Expansion of  $X, Y, Z, L, M, N$  for a single rotor helicopter is studied in [1,3,10,11,12]. We pass this stage because evaluating rotorcraft forces and moments are wide area of study. We will use only results that we have obtained.

Design procedure of AFCS is based on linear quadratic optimal control problem. At this stage, nonlinear flight dynamics will be linearized and control law will be designed on linear flight dynamic model. To guarantee the stability at any flight speed and altitude control gains will be scheduled for flight speed and altitude by flight computer from data tables. We would like to point that simulations of AFCS will be performed on nonlinear flight dynamics model.

The linear form of above equation of motions (1)-(3) describing rigid body motion of helicopter is of the form:

$$\dot{x} = [A]x + [B]\delta \quad (5)$$

where  $x$  is the perturbations from trim of the states variables of longitudinal motion:  $u_B, w_B, q_B, \theta_B$  and lateral motion:  $v_B, p_B, \phi_B, r_B, \psi_B$ ;  $\delta$  is the deviation from trim control positions of longitudinal motion  $\delta_c, \delta_{1s}$  and lateral motion  $\delta_{lc}, \delta_p$ . The elements of the  $A$  and  $B$  matrices consist of inertial and gravitational terms that can be obtained analytically from the equation of motion (1)-(3) and partial derivatives formed from aerodynamics forces and moments. The force and moment derivatives can be obtained by considering both position and negative perturbation from trim as [1,9]:

$$X_{u_B} = \frac{\partial X}{\partial u_B} \cong \frac{X(u_0 + \Delta u_B) - X(u_0 - \Delta u_B)}{2\Delta u_B} \quad (6)$$

Normalized stability and control derivatives for longitudinal motion are  $x_i = X_i/m, z_i = Z_i/m, m_i = M_i/I_{yy}$ , where  $i = u_B, w_B, q_B, \delta_c, \delta_{1s}$ . For lateral motion stability and control derivatives are normalized as  $y_j = Y_j/m, \tilde{l}_j = (I_{zz}L_j + I_{xz}N_j)/I_c, \tilde{n}_j = (I_{xz}L_j + I_{zz}N_j)/I_c$ , where  $j = v_B, p_B, r_B, \delta_{lc}, \delta_p$  and  $I_c = I_{xx}I_{zz} - I_{xz}^2$ . These derivatives are calculated for considered helicopter in [1] for many trim conditions. At the end of the paper in Table 2 we give some stability and control derivatives for prototype helicopter model at different flight speeds and altitudes. Also, corresponding stability and control derivatives that appear in this paper can be easily calculated from nonlinear flight dynamics model for any trim conditions in the bounds of 0 to 70 m/s forward speed and 0 to 10,000 ft of flight altitude with steps size of 5 m/s of forward speed and 2,500 ft of altitude.

### 2.1 Speed Hold Problem

For speed hold problem now consider linearized the set of equation witch are enough to describe longitudinal flight dynamics of the helicopter [6]:

$$\dot{u}_B = x_u u_B + x_w w_B + (z_q - w_0) q_B - g \cos \gamma_0 + x_{\delta_c} \delta_c + x_{\delta_{1s}} \delta_{1s} \quad (7)$$

$$\dot{w}_B = z_u u_B + z_w w_B + (z_q + u_0) q_B - g \sin \gamma_0 + z_{\delta_c} \delta_c + z_{\delta_{1s}} \delta_{1s} \quad (8)$$

$$\dot{q}_B = m_u u_B + m_w w_B + m_q q_B + m_{\delta_c} \delta_c + m_{\delta_{1s}} \delta_{1s} \quad (9)$$

$$\dot{\theta}_B = q_B \quad (10)$$

The state space form is:

$$\begin{aligned} \dot{x}_{SH}(t) &= A_{SH} x_{SH}(t) + B_{SH} \delta_{SH}(t) \\ y_{SH}(t) &= C_{SH} x_{SH}(t) \end{aligned} \quad (11)$$

where the state vector is  $x_{SH}(t)=[u_B \ w_B \ q_B \ \theta_B]^T$ , the control vector is  $\delta_{SH}(t)=[\delta_c \ \delta_{1s}]^T$ ,  $C_{SH}$  is unit matrix, and

$$A_{SH} = \begin{bmatrix} x_u & x_w & x_q - w_0 & -g \cos \gamma_0 \\ z_u & z_w & z_q + u_0 & -g \sin \gamma_0 \\ m_u & m_w & m_q & 0 \\ 0 & 0 & 1 & 0 \end{bmatrix} \quad (12)$$

$$B_{SH} = \begin{bmatrix} x_{\delta_c} & x_{\delta_{1s}} \\ z_{\delta_c} & z_{\delta_{1s}} \\ m_{\delta_c} & m_{\delta_{1s}} \\ 0 & 0 \end{bmatrix} \quad (13)$$

The stability of longitudinal flight dynamics can be determined by calculation of the eigenvalues of the system matrix  $\lambda(A_{SH})$ . Eigenvalues are illustrated in Figure 3 for considered flight envelope. There are many roots at rights side of imaginary axis which means that open-loop longitudinal dynamics are unstable.

### 2.2 Height Hold Problem

For height/altitude hold system linear height dynamics as given below are included to the linear longitudinal dynamics described in previous subsection by (12)-(13) as [6]:

$$\dot{h} = -w_B + u_0 \theta_B \quad (14)$$

Therefore, the state vector can be rewritten as  $x_{SH}(t)=[u_B \ w_B \ q_B \ \theta_B \ h]^T$ . Then, system and control distribution matrices can be formed as:

$$A_{SH} = \begin{bmatrix} x_u & x_w & x_q - w_0 & -g c \gamma_0 & 0 \\ z_u & z_w & z_q + u_0 & -g s \gamma_0 & 0 \\ m_u & m_w & m_q & 0 & 0 \\ 0 & 0 & 1 & 0 & 0 \\ 0 & -1 & 0 & u_0 & 0 \end{bmatrix} \quad (15)$$

$$B_{SH} = \begin{bmatrix} x_{\delta_c} & x_{\delta_{1s}} \\ z_{\delta_c} & z_{\delta_{1s}} \\ m_{\delta_c} & m_{\delta_{1s}} \\ 0 & 0 \\ 0 & 0 \end{bmatrix} \quad (16)$$

The eigenvalues of height hold dynamics are given in Figure 3. As seen from the figure so many eigenvalues are the right side of imaginary axis and the worst situation is that some of them have greater values which mean that those modes cannot be stabilized by a human pilot.

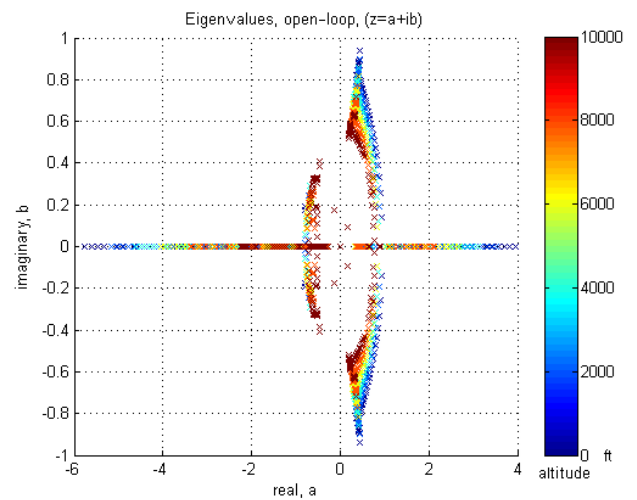


Figure 3 Eigenvalues of open-loop longitudinal helicopter flight dynamics.

### 2.3 Heading Hold Problem

Heading of rotorcraft is determined by lateral flight dynamics. The set of equation which describes lateral flight dynamics are [6]:

$$\dot{y}_B = y_v v_B + (y_r - u_0) r_B + (y_p - w_0) p_B + g c \phi_0 c \gamma_0 + y_{\delta_{1c}} \delta_{1c} + y_{\delta_p} \delta_p \quad (17)$$

$$\dot{p}_B = \tilde{l}_v v_B + \tilde{l}_p p_B + \tilde{l}_r r_B + \tilde{l}_{\delta_{1c}} \delta_{1c} + \tilde{l}_{\delta_p} \delta_p \quad (18)$$

$$\dot{r}_B = \tilde{n}_v v_B + \tilde{n}_p p_B + \tilde{n}_r r_B + \tilde{n}_{\delta_{1c}} \delta_{1c} + \tilde{n}_{\delta_p} \delta_p \quad (19)$$

$$\dot{\phi}_B = p_B + c \phi_0 t \theta_0 r_B \quad (20)$$

$$\dot{\psi}_B = c \phi_0 s c \theta_0 r_B \quad (21)$$

The state space form is:

$$\begin{aligned} \dot{x}_{HH}(t) &= A_{HH} x_{HH}(t) + B_{HH} \delta_{HH}(t) \\ y_{HH}(t) &= C_{HH} x_{HH}(t) \end{aligned} \quad (22)$$

where the state vector is  $x_{SH}(t)=[v_B p_B \phi_B r_B \psi_B]^T$ , the control vector is  $\delta_{HH}(t)=[\delta_{lc} \delta_p]^T$ , and

$$A_{HH} = \begin{bmatrix} y_v & y_p + w_0 & g c \phi_0 c \gamma_0 & y_r - u_0 & 0 \\ \tilde{l}_v & \tilde{l}_p & 0 & \tilde{l}_r & 0 \\ 0 & 1 & 0 & c \phi_0 t \theta_0 & 0 \\ \tilde{n}_v & \tilde{n}_p & 0 & \tilde{n}_r & 0 \\ 0 & 0 & 0 & c \phi_0 s c \theta_0 & 0 \end{bmatrix} \quad (23)$$

$$B_{HH} = \begin{bmatrix} y_{\delta_{lc}} & y_{\delta_p} \\ \tilde{l}_{\delta_{lc}} & \tilde{l}_{\delta_p} \\ 0 & 0 \\ \tilde{n}_{\delta_{lc}} & \tilde{n}_{\delta_p} \\ 0 & 0 \end{bmatrix} \quad (24)$$

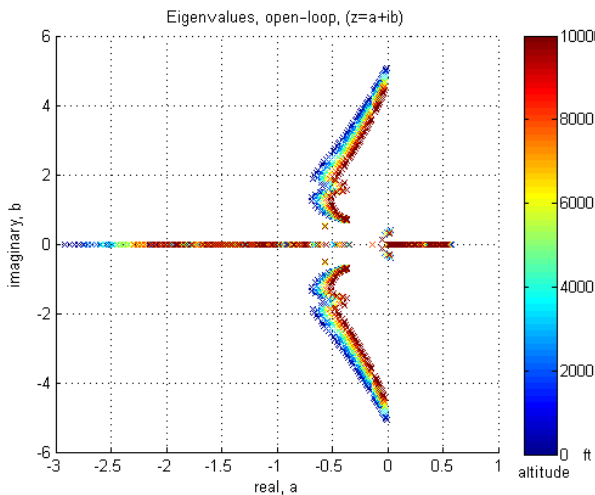


Figure 4 Eigenvalues of open-loop lateral helicopter flight dynamics.

The stability of lateral dynamics system can be obtained by calculation of the eigenvalues of the system matrix  $A_{HH}$ . Eigenvalues are illustrated in Figure 4 for considered flight envelope. There are many roots at rights side of imaginary axis which means that open-loop longitudinal dynamics are unstable.

### 3 Design of Automatic Flight Control System (AFCS)

Typically, SAS, autopilot and flight director systems and modes of operations are lumped together and referred to as an Automatic Flight Control System (AFCS). There can be various combinations of single and dual AFCS installations available for a particular helicopter model. In this paper we have considered single mode. The LQ optimal control law for AFCS is designed to reduce pilot workload,

improve mission reliability and enhance safety of flight.

#### 3.1 LQ Optimal Control Law

Consider that helicopter flight dynamics are described with linear set of equations like (15)-(16) or (23)-(24). To achieve an optimal condition a performance measure to be minimized should be defined [8]:

$$J = \frac{1}{2} \int_0^{\infty} (x^T(t)Q(t)x(t) + \delta^T(t)R(t)\delta(t)) dt \quad (25)$$

where  $Q$  is a real symmetric positive semi-definite matrix,  $R$  is a real symmetric positive definite matrix,  $x$  and  $\delta$  are states and control vectors, respectively. In the design process, it is assumed that the states and controls are not bounded. However, control inputs are bounded due to physical limitation of the swash plate mechanism and also states of the system are bounded because of aerodynamic rules and performance of power-plant. Here, the aim is to maintain the state vector close to the origin without an excessive expenditure of control effort. So, the optimal control law is linear and it is formed as a combination of the system as [8]:

$$\delta^*(t) = -R^{-1}B^T Fx^*(t) = -Kx^*(t) \quad (26)$$

where  $F$  is the solution of following Algebraic Riccati Equation (ARE):

$$A^T F + FA + Q - FBR^{-1}BF = 0 \quad (27)$$

And the optimal cost of performance index can be calculated from:  $J = 0.5x^T(0)Kx(0)$ .

The stability of the closed-loop system can be determined by calculation of the eigenvalues of the closed-loop system matrix  $A - BR^{-1}B^T F$  or  $(A - BK)$  according to the optimal control law (26).

#### 3.2 Gain Scheduled LQ Optimal Control Law

Gain scheduling simply means changing values of control matrix according to predefined conditions. In this paper, the control law is calculated for each trim points considered in flight envelope. In other words, the control matrix  $K$  is determined from forward speed and flight altitudes as:

$$\delta^*(h,u,t) = -K(h,u)x^*(t) \quad (28)$$

In this paper we have obtained surfaces for each gain of control matrix  $K$ .

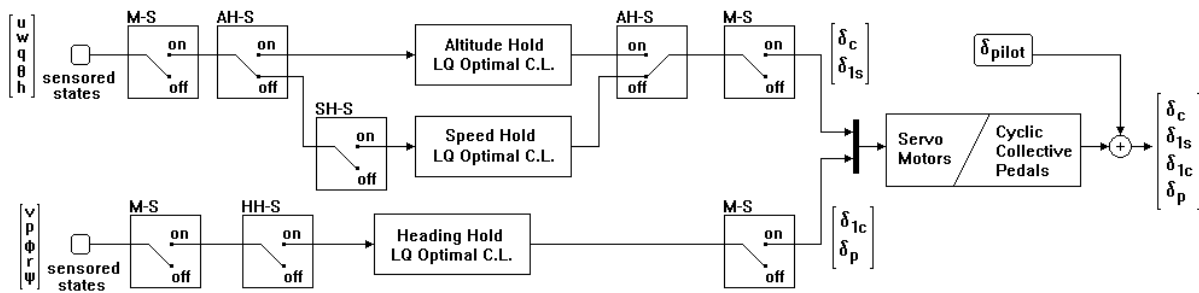


Figure 5 Block scheme of proposed AFCS

3.3 Gain Scheduled Speed Hold AFCS

The proposed LQ optimal control law for speed hold AFCS is considered as:

$$\delta^* = \begin{bmatrix} \delta_c \\ \delta_{1s} \end{bmatrix} = -K_{SH}(h,u)x_{SH}^*(t) \tag{29}$$

where  $K_{SH,ij}(h,u)$  is the scheduled control matrix which elements are selected from Figure 9. In flight computer these plots are coded as look-up tables. The eigenvalues of Speed Hold AFCS are illustrated in Figure 6. As seen from figure closed-loop eigenvalues are at left side of imaginary axis which means the system is stable. After speed hold is turned on, reference value is selected to be current forward flight speed. Therefore, longitudinal dynamics of the rotorcraft is stabilized near selected forward speed by selection of proper gains from look-up tables in (30) and therefore hands free flight is achieved.

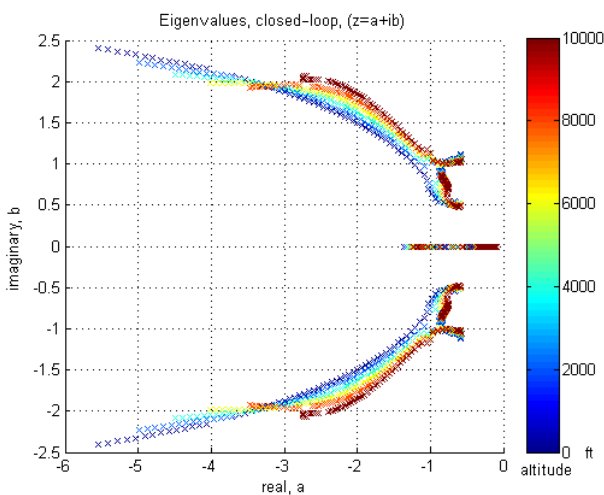


Figure 6 Eigenvalues of closed-loop speed hold system

3.4 Gain Scheduled Height Hold AFCS

Similarly to previous control law height hold is formed as:

$$\delta^* = \begin{bmatrix} \delta_c \\ \delta_{1s} \end{bmatrix} = -K_{AH}(h,u)x_{AH}^*(t) \tag{30}$$

where  $K_{AH,ij}(h,u)$  is the scheduled control matrix which elements are selected from Figure 10. Switching height hold on selects reference values to be current forward speed and altitude. If speed hold is on when height hold is switched on then control law for longitudinal motion is replaced with height hold control algorithm (31). Therefore, longitudinal dynamics of the rotorcraft is stabilized near selected forward speed and flight altitude. The eigenvalues of Speed Hold AFCS are illustrated in Figure 7. O, the stability of the closed-loop system is graphically shown. All real parts of eigenvalues of height hold system are negative signed with enough damping values.

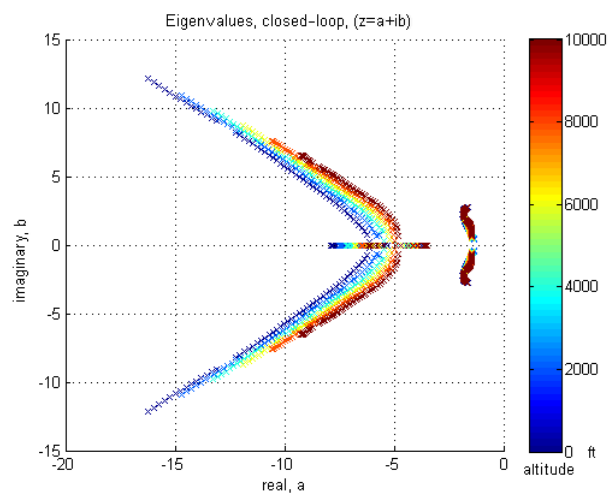


Figure 7 Eigenvalues of closed-loop height hold system.

### 3.5 Gain Scheduled Heading Hold AFCS

The proposed LQ optimal control law for heading hold AFCS is considered similarly to previous ones as:

$$\delta^* = \begin{bmatrix} \delta_{1c} \\ \delta_p \end{bmatrix} = -K_{HH}(h,u)x_{HH}^*(t) \quad (31)$$

where  $K_{HH,ij}(h,u)$  is the scheduled control matrix which elements are selected from Figure 11. In flight computer these plots are coded as look-up tables. The eigenvalues of Heading Hold AFCS are illustrated in Figure 8. As seen, all eigenvalues of closed-loop system for bounded flight condition are pushed to the left side of imaginary axis. This plot illustrates graphically the stability of the system.

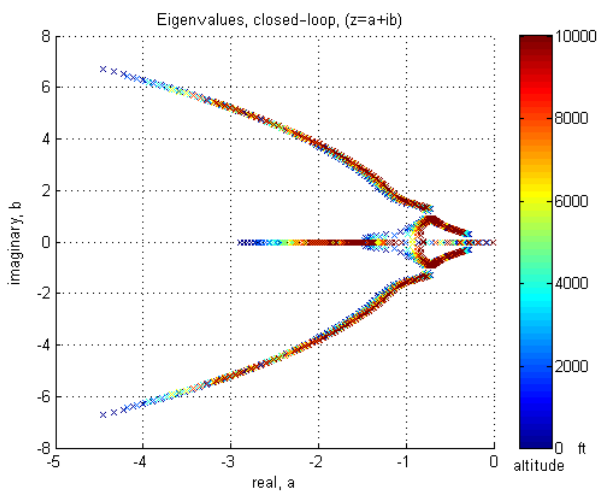


Figure 8 Eigenvalues of closed-loop heading hold system.

## 4 Simulations

After design of AFCS we need to test its performance and time responses. For this purpose we have considered nonlinear rotorcraft dynamics model of prototype helicopter given in [1]. The mathematical model is built in Matlab-Simulink environment and top view of its block diagram is given in Figure 12. Time responses of pure rotorcraft dynamics or disabled (off mode) of AFCS are shown in figure 13. As seen from the figure the unstable nature of rotorcraft pushes state variables away from steady state situation after 4 seconds. This time is sufficient for the pilot to take a control action to stabilize the rotorcraft. To improve mission reliability, enhance safety of flight without excessive control inputs and reduce pilot workload AFCS is enabled for different operating cases and maneuvers.

Time responses of maneuvers rejecting 5 m/s (9.72 knots) vertical and sideward winds with 5 seconds duration at sea level and 30 m/s (58.32 knots) forward flight speed are given in Figure 14 and 15, respectively. In this case, only master switch of AFCS is on. The disturbance wind effects are rejected with high damping pitch and roll rates for both cases. However rotorcraft model is losing 30 m of altitude and pushed 25 m to sideward for each maneuver.

Forward speed correction maneuver at sea level and 30 m/s (58.32 knots) forward flight speed is given in Figure 16. The optimal control algorithm eliminates 3 m/s forward speed error in a couple of seconds with high damping attitude rates where only master switch of AFCS is on. On the other hand, attitude angles reach steady state in 15 seconds with a comfortable maneuver.

Time responses for total 7.1 m/s (13.8 knots) crosswind rejection at sea level and 30 m/s (58.32 knots) forward flight speed when AFCS master, speed hold, height hold, and heading hold switches are engaged are given in Figure 17. The distributive crosswind with 5 seconds duration is eliminated in 15 seconds. LQ optimal control algorithm provides high damping roll, pitch and yaw rates. But roll angle seems to exhibit damped oscillation for a while during stabilization because of the 7.1 m/s crosswind. For this disturbance rejection maneuver only collective inputs appears to provide a little bit high control values in arrange of 15 degrees to keep rotorcraft at desired flight altitude, where the rest control inputs changes in 2-3 degrees.

## 5 Conclusion

In this paper, we have introduced nonlinear rigid body dynamics for rotorcraft mathematical model. Then we have linearized helicopter flight dynamics to design a gain scheduled LQ optimal control system to reduce pilot workload, improve mission reliability and enhance safety of flight without excessive control inputs. We have designed our AFCS to stabilize helicopter flight dynamics and maintain desired flight speed, altitude and heading as gain scheduled where gains of feedback matrix are selected with flight speed and altitude from look-up tables coded in flight computer.

Stability analyze is performed graphically by plotting eigenvalues both for open and closed-loop systems in considered flight envelope which bounds are 0 to 70 m/s forward speed and 0 to 10,000 ft of flight altitude. Proposed LQ optimal control law

have pushed eigenvalues to the left side of imaginary axis for all design conditions.

Proposed control laws are designed on linear flight dynamics however they are evaluated in nonlinear flight dynamics mathematical model of the prototype helicopter. Simulation results illustrate effectiveness of evaluated method and techniques.

#### References:

- [1] E. Abdulhamitbilal, *ITU-Light Commercial Helicopter flight dynamics, stability analysis, and interconnected control systems design*, ITU-Library, Istanbul, 2010.
- [2] T. F. Hanson, *A Designer Friendly Handbook of Helicopter Rotors*, ideasalacarte.com, 1998.
- [3] J.J. Howlett, *UH-60A Black Hawk Engineering Simulation Program: Volume I – Mathematical Model*, NASA CR 166309, 1981.
- [4] E. Abdulhamitbilal, E.M. Jafarov, and L. Güvenç, Gain Scheduled LQ Optimal Control of a Parametric Light Commercial Helicopter Model at Sea Level. *Proceedings of ACMOS'07, 9th WSEAS International Conference on Automatic Control, Modeling and Simulation*, June 27-29, 2007, Istanbul, Turkey,
- [5] C.Y. Huang, R. Celi, I-C. Shih, Reconfigurable flight control systems for a tandem helicopter, *Journal of American Helicopter Society*, vol. 44, pp. 50-62.
- [6] D. McLean, *Automatic Flight Control Systems*, Prentice Hall, London, 1990.
- [7] B.L. Stevens, F.L. Lewis, *Aircraft Control and Simulation*, John Wiley & Sons, Inc., 1992.
- [8] D.E. Kirk, *Optimal Control Theory*, Prentice Hall, New Jersey, 1970.
- [9] K.J. Aström, B. Wittenmark, *Adaptive Control*, Addison-Wesley, New Jersey, 1995.
- [10] W. Johnson, *Helicopter Theory*. Dover Publications Inc, New York, 1994.
- [11] R.W. Prouty, *Helicopter Performance, Stability, and Control*. Krieger Publishing, Florida, 1995.
- [12] A.R.S. Bramwell, G.T. Sutton Done, D. Balmford, *Bramwell's Helicopter Dynamics*, 2nd Edition, AIAA, Virginia, 2001
- [13] M.D. Takahashi, Rotor-state feedback in the design of flight control laws for a hovering helicopter, *Journal of American Helicopter Society*, vol. 39, pp. 50-6270.
- [14] R.M. McKilip Jr., T.A. Perri, Helicopter flight control system design and evaluation using controller inversion techniques, *Journal of American Helicopter Society*, vol. 37, pp. 66-74.
- [15] J.N. Rozak, A. Ray, Robust multivariable control of rotorcraft in forward flight, *Journal of American Helicopter Society*, vol. 42, pp. 149-160.
- [16] I. Postlethwaite, A. Smerlas, D.J. Walker, A.W. Gubbels, S.W. Baillie, M.E. Strange, J. Howitt,  $H_\infty$  control of the NRC Bell 205 fly-by-wire helicopter, *Journal of American Helicopter Society*, vol. 44, pp. 276-284.
- [17] Y. Isik, Pitch rate damping of an aircraft by fuzzy and classical PD control, *WSEAS Transactions on Systems and Control 5 (7)*, 2010, pp. 581-590.
- [18] J.-M. Lin, P.-K. Chang, Ziegler-Nichols PID controller based intelligent fuzzy control of a SPM system design, *WSEAS Transactions on Systems and Control 5 (10)*, 2010, pp. 847-857.

Table 2 Some stability and control derivatives of prototype helicopter

$U_0$	$h$	$T$	$GW$							
0m/s	0ft	288K	2027kg							
$\phi$	$\theta$	$\psi$	$\theta_c$	$\theta_{1s}$	$\theta_{1c}$	$\theta_p$				
-0.0262	0.0538		0.13.6447	-0.0034	-0.1105	9.5916				
$U$	$V$	$Q$	$V$	$P$	$R$	$dc$	$d1s$	$d1c$	$dp$	
X	0	-0.0047	0.0000	-0.0003	-0.0061	0.0013	0.0938	0.0588	-0.0442	-0.0002
Z	0.0242	0.0779	0.2786	0.0065	0.2755	-0.2800	-1.7419	-0.0045	-0.0006	0
M	-0.0008	0.0042	-0.0101	0.0108	0.0004	0.0158	-0.0808	-0.7503	-3.9854	0.0023
Y	-0.2442	-0.1808	0	0.0050	0.0138	0.4203	-0.0466	0.0443	0.0587	0.0744
L	-0.0363	-0.0820	-0.1529	0.0404	-0.6056	1.0936	-0.0947	-12.0167	0.4145	0.0726
N	0.0877	0.0673	0.0063	-0.0026	0.0305	-0.9925	0.2979	0.4976	-0.0011	-0.2150
30m/s	0ft	288K	2027kg							
0.0067	0.0404		0.12.0081	-2.0898	1.0178	2.9790				
0.0017	0.0762	-0.0238	-0.0028	0.0159	-0.0053	0.1755	0.1640	-0.0350	0.0023	
0.0019	-0.9037	0.0190	0.0237	0.0100	-0.0006	-2.1228	-0.7802	-0.2266	-0.0000	
0.0869	0.0474	-0.2397	-0.0247	0.0305	-0.0136	0.3624	-0.9286	-3.9284	0.0062	

0.0045	-0.0629	0.0798	-0.0292	-0.1612	0.1856	-0.0511	0.0628	0.1194	0.0564
-0.8048	-1.0501	2.5507	0.0064	-1.2738	0.6285	-5.0258	-12.416	0.7047	-0.0759
0.0211	-0.0639	-0.1142	0.0992	-0.0243	-0.3409	0.3667	0.5662	0.0558	-0.2224

50m/s	0ft	288K	2027kg						
0.0010	0.0212	0	13.0776	-3.8261	2.0694	2.7301			

-0.0073	0.1136	-0.0205	-0.0044	0.0516	-0.0076	0.2428	0.1894	-0.0178	0.0059
0.0636	-1.0784	-0.1243	0.0402	0.0210	-0.0011	-2.3899	-1.2139	-0.2958	-0.0000
0.1108	0.1422	-0.3302	-0.0399	0.1148	-0.0193	0.7565	-0.8434	-3.8725	0.0147
0.0127	-0.1080	0.1366	-0.0435	-0.2722	0.0864	-0.0828	0.0780	0.1040	0.0732
-0.7513	-2.0256	2.9565	-0.0339	-2.0840	0.3336	-8.4355	-12.868	0.3564	-0.0818
0.0184	-0.0618	-0.1202	0.1286	-0.0213	-0.1402	0.4858	0.5850	0.1714	-0.2825

70m/s	0ft	288K	2027kg						
-0.0216	-0.0059	0	16.1051	-7.0568	4.1965	3.4213			

-0.0207	0.1657	-0.0050	-0.0045	0.0770	-0.0002	0.3007	0.2051	0.0145	0.0079
0.1100	-1.2599	-0.2410	0.0571	0.0334	-0.0006	-2.5473	-1.6040	-0.2958	0.0000
0.1873	0.3377	-0.5433	-0.0510	0.1813	-0.0030	1.2968	-0.5709	-3.7399	0.0196
0.0285	-0.1486	0.1752	-0.0561	-0.3828	-0.0145	-0.0792	0.1145	0.0400	0.0826
-0.8880	-3.2134	3.7702	-0.0898	-2.8802	-0.0892	-11.599	-13.416	-0.0705	-0.1056
-0.0113	-0.0323	-0.0691	0.1457	-0.0083	0.0049	0.5190	0.5609	0.4245	-0.3251

0m/s	10000ft	288K	2027kg						
-0.0290	0.0540	0	15.4939	-0.0078	-0.1541	12.4208			

0	-0.0036	0.0000	-0.0002	-0.0054	0.0011	0.0736	0.0410	-0.0480	-0.0002
0.0243	0.0760	0.2797	0.0056	0.2903	-0.2810	-1.3631	-0.0040	0.0013	0
-0.0009	0.0042	-0.0102	0.0093	0.0030	0.0142	-0.0631	-0.7423	-2.8190	0.0023
-0.2447	-0.1389	0	0.0045	0.0119	0.3183	-0.0358	0.0481	0.0409	0.0588
-0.0364	-0.0789	-0.1535	0.0361	-0.6516	0.9018	-0.0863	-8.8377	0.5240	0.0575
0.0878	0.0523	0.0064	-0.0023	0.0318	-0.7377	0.2764	0.3659	-0.0077	-0.1701

30m/s	10000ft	288K	2027kg						
0.0060	0.0457	0	13.7738	-2.7966	0.9509	4.1949			

0.0061	0.0568	-0.0268	-0.0015	0.0010	0.0002	0.1340	0.1229	-0.0480	-0.0001
-0.0122	-0.6782	0.0490	0.0174	0.0073	-0.0004	-1.5853	-0.5744	-0.1214	-0.0000
0.0258	-0.0052	-0.0765	-0.0169	-0.0037	-0.0001	0.0296	-0.8594	-2.7881	0.0006
0.0066	-0.0439	0.0526	-0.0199	-0.1369	0.1514	-0.0213	0.0663	0.0920	0.0379
-0.8125	-0.7843	2.4114	0.0149	-1.0610	0.5475	-3.6581	-9.0889	0.7369	-0.0794
0.0222	-0.0621	-0.1113	0.0717	-0.0067	-0.2656	0.3208	0.4307	0.0234	-0.1612

50m/s	10000ft	288K	2027kg						
0.0086	0.0350	0	14.7539	-4.9817	1.8624	3.6433			

-0.0011	0.0843	-0.0248	-0.0033	0.0326	-0.0053	0.1841	0.1374	-0.0370	0.0039
0.0450	-0.8017	-0.0776	0.0294	0.0153	-0.0011	-1.7654	-0.8674	-0.1647	-0.0001
0.0347	0.0184	-0.1258	-0.0297	0.0686	-0.0130	0.1314	-0.8276	-2.7668	0.0098
0.0117	-0.0732	0.0917	-0.0315	-0.2024	0.0738	-0.0317	0.0796	0.0861	0.0503
-0.7438	-1.5002	2.6436	-0.0208	-1.5463	0.2904	-6.0508	-9.2135	0.5336	-0.0755
0.0246	-0.0609	-0.1236	0.0943	-0.0115	-0.1187	0.4318	0.4513	0.0886	-0.2028

70m/s	10000ft	288K	2027kg						
0.0079	0.0253	0	17.3899	-8.6025	3.4434	4.7435			

-0.0087	0.1048	-0.0169	-0.0036	0.0508	-0.0013	0.2229	0.1617	-0.0056	0.0055
0.0786	-0.8472	-0.1613	0.0415	0.0247	-0.0015	-1.8139	-1.2095	-0.2690	-0.0001
0.0699	0.0356	-0.2370	-0.0388	0.1106	-0.0042	0.2178	-0.6807	-2.4986	0.0139
0.0226	-0.0910	0.1178	-0.0419	-0.2839	0.0029	-0.0115	0.0938	0.0339	0.0556
-0.7396	-2.3294	2.9673	-0.0629	-2.1327	-0.0024	-7.9537	-8.9520	0.1565	-0.1021
0.0129	-0.0080	-0.1141	0.1100	-0.0006	-0.0140	0.5511	0.4497	0.2019	-0.2328

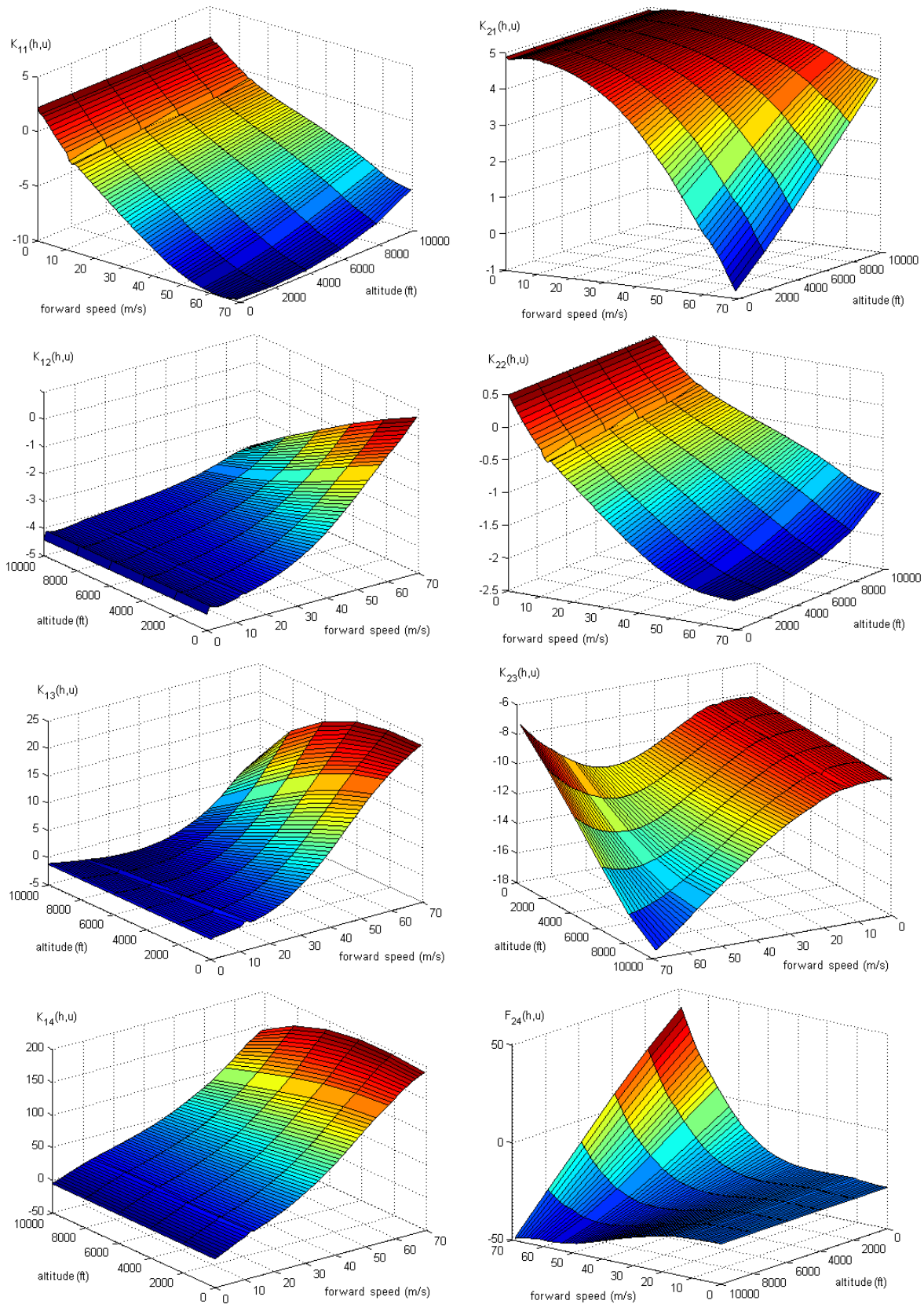
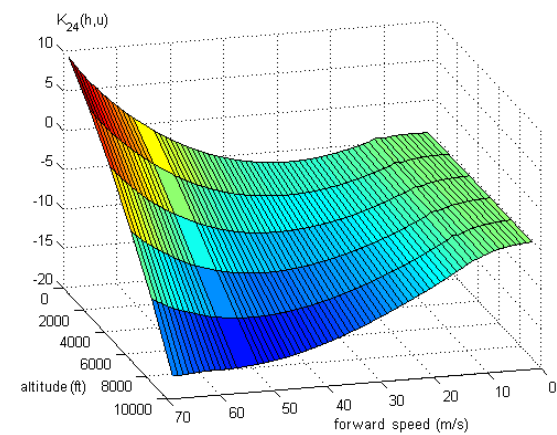
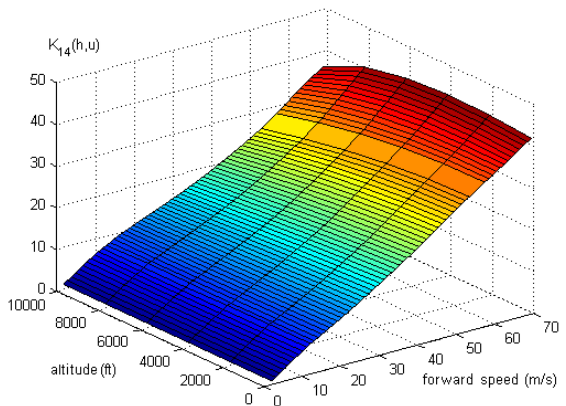
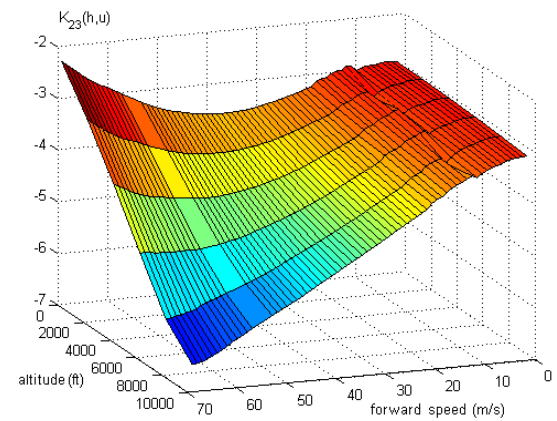
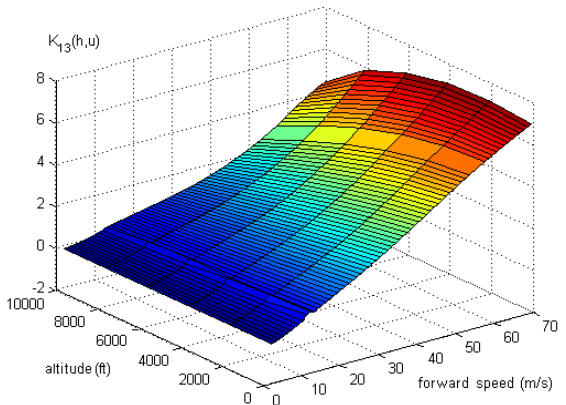
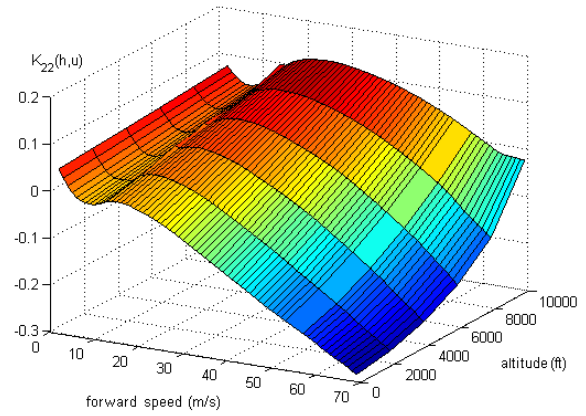
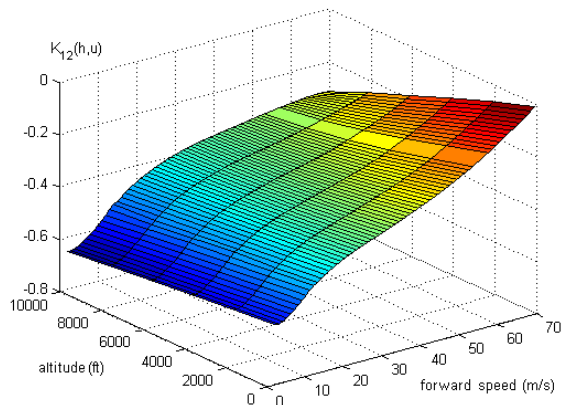
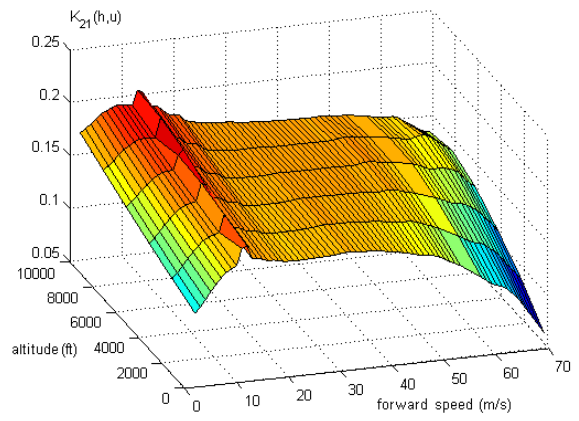
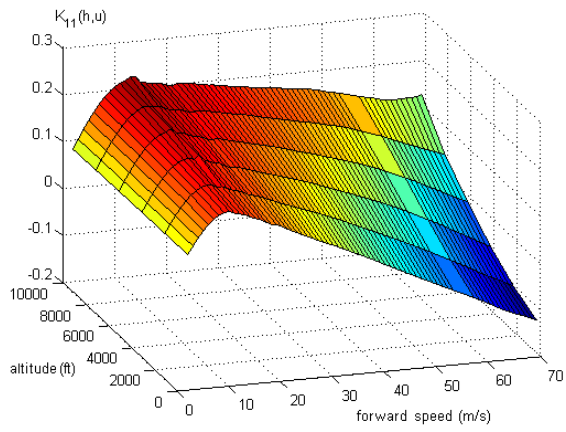


Figure 9 Gain scheduling surfaces of speed hold feedback matrix gain,  $K_{SH}(h,u)$ .



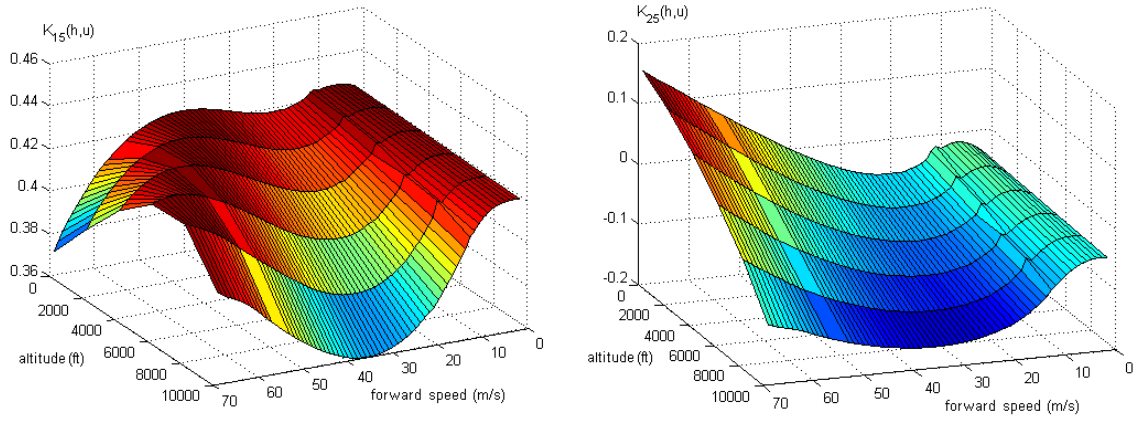
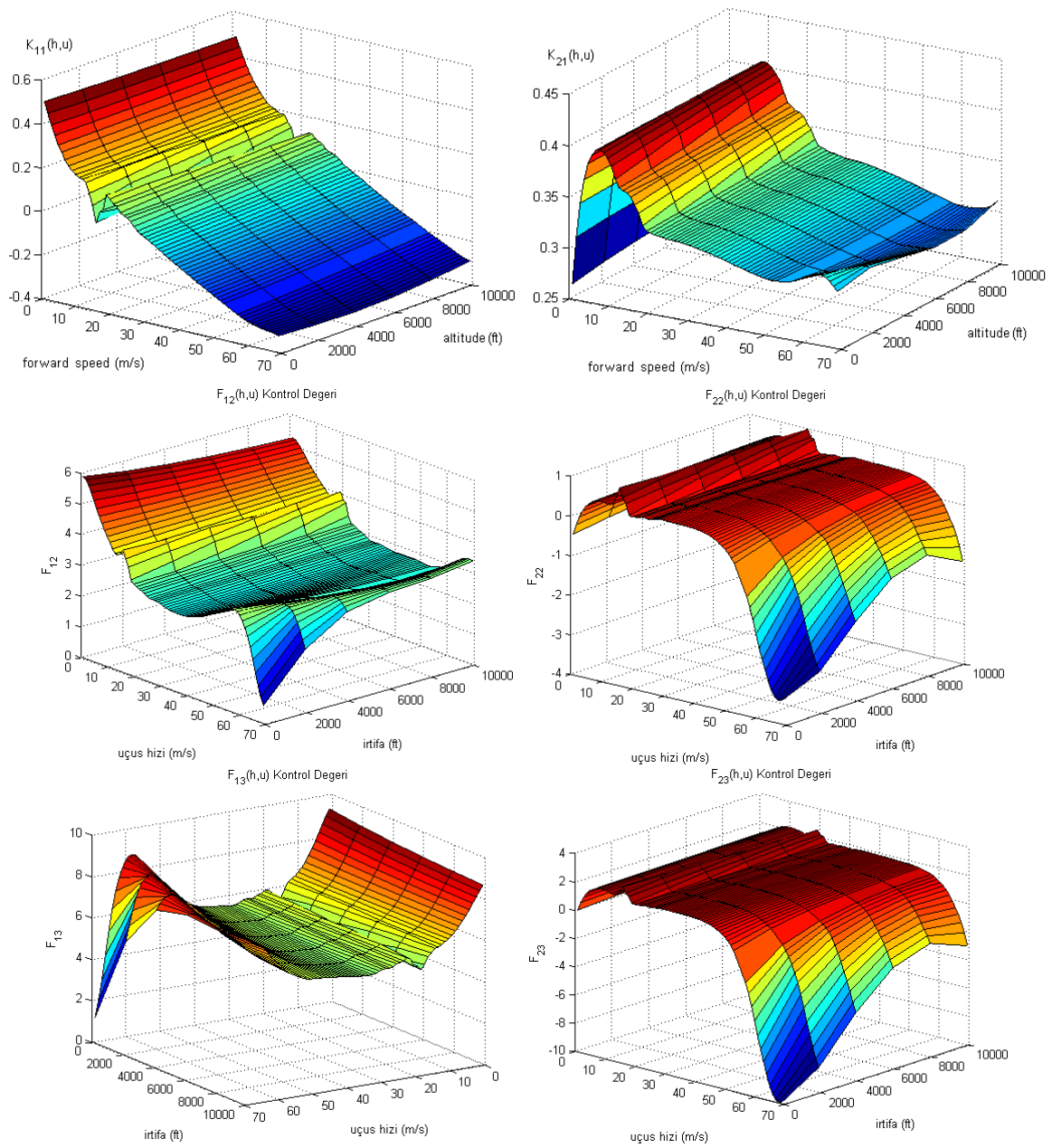


Figure 10 Gain scheduling surfaces of height hold feedback matrix gain,  $K_{AH}(h,u)$ .



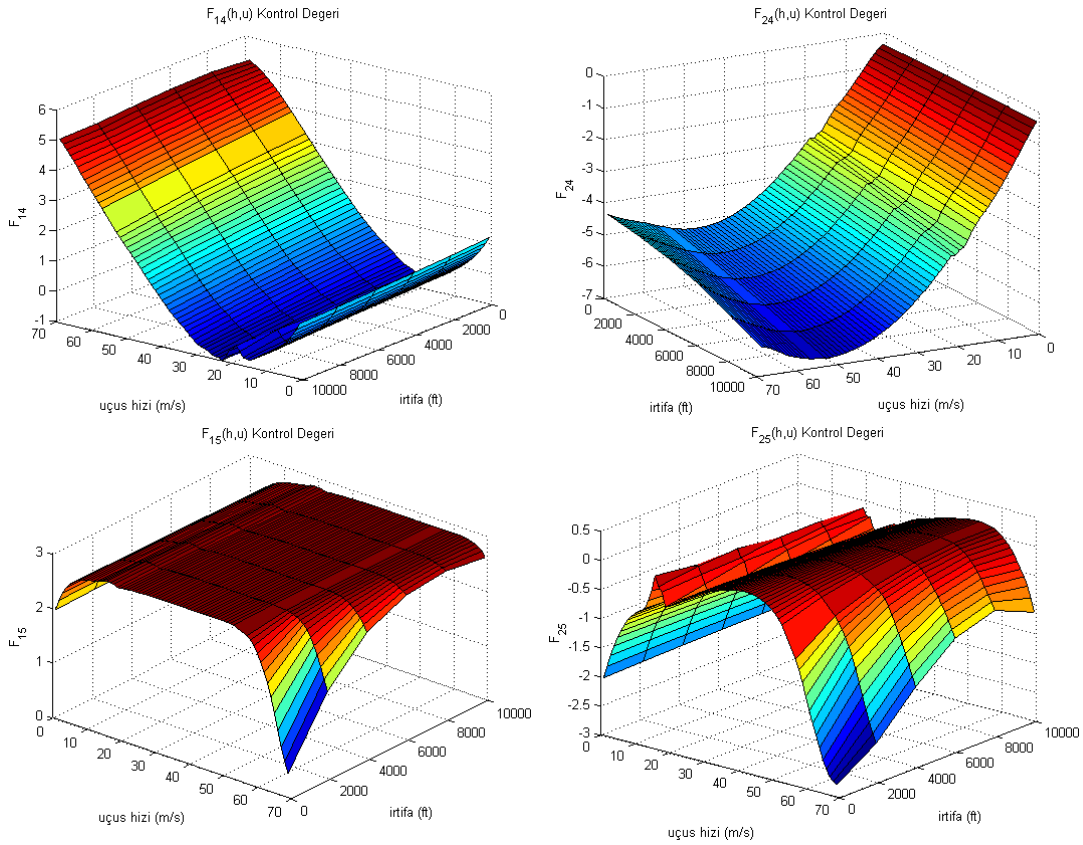


Figure 11 Gain scheduling surfaces of heading hold feedback matrix gain,  $K_{HH}(h,u)$ .

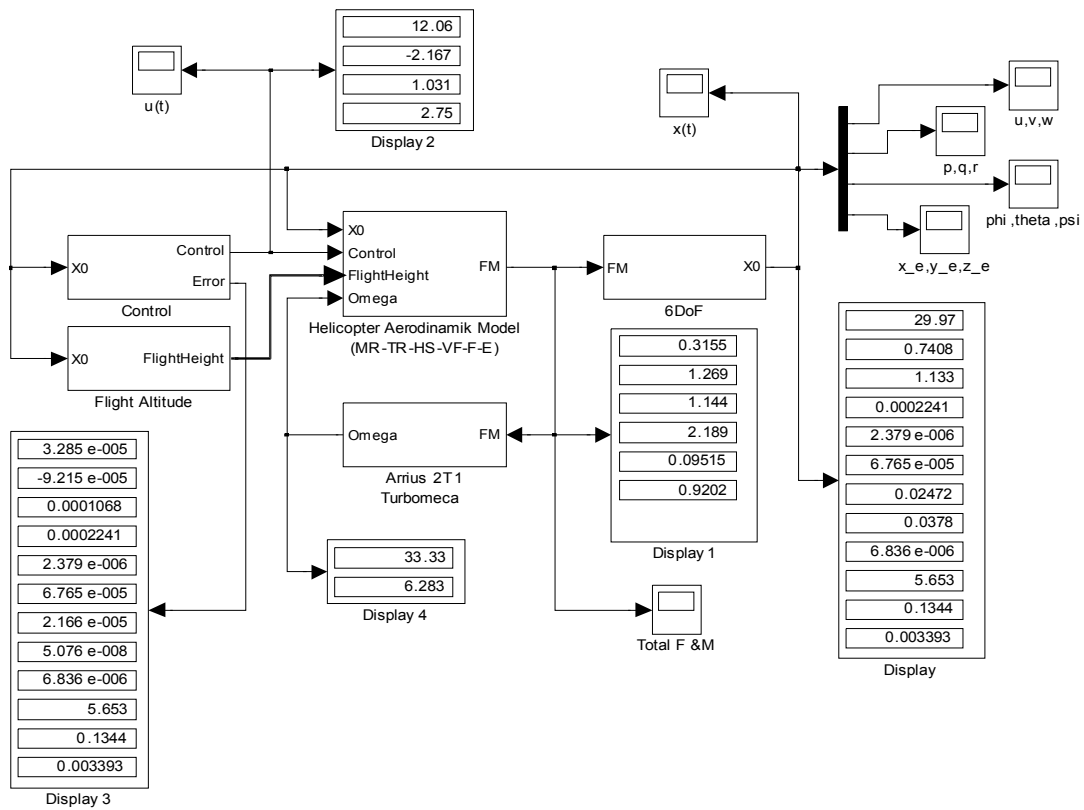


Figure 12 Block diagram of nonlinear flight dynamics of prototyped helicopter

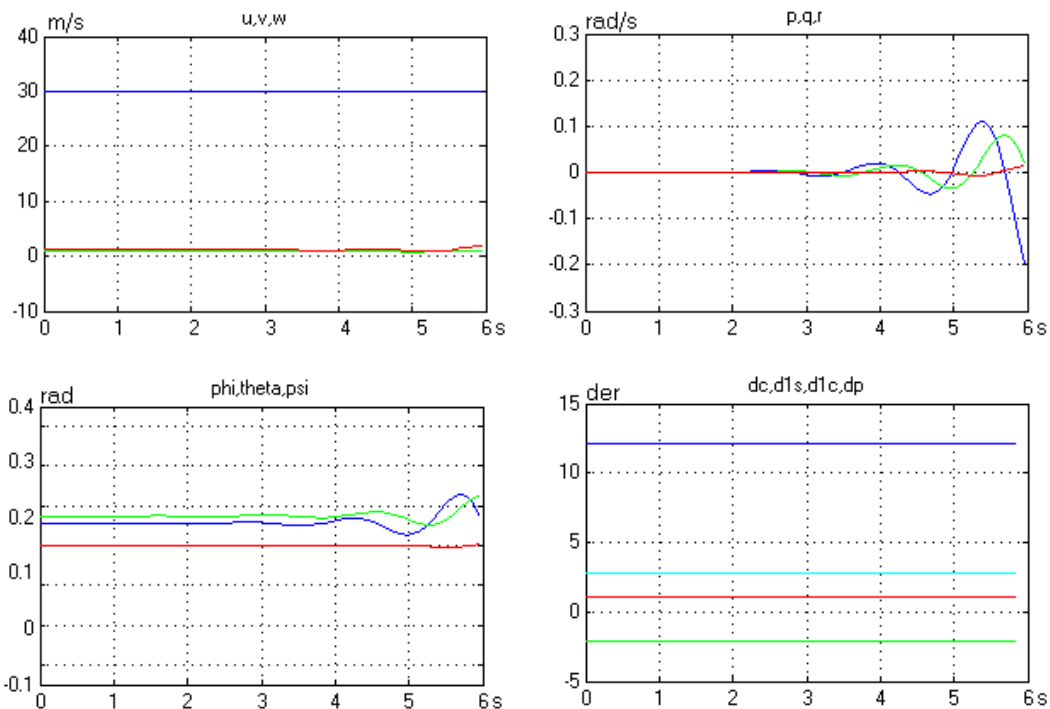


Figure 13 Time responses of nonlinear model for a trim condition ( $h = 0\text{ft}$ ,  $u = 30\text{m/s}$ ): AFCS is off.

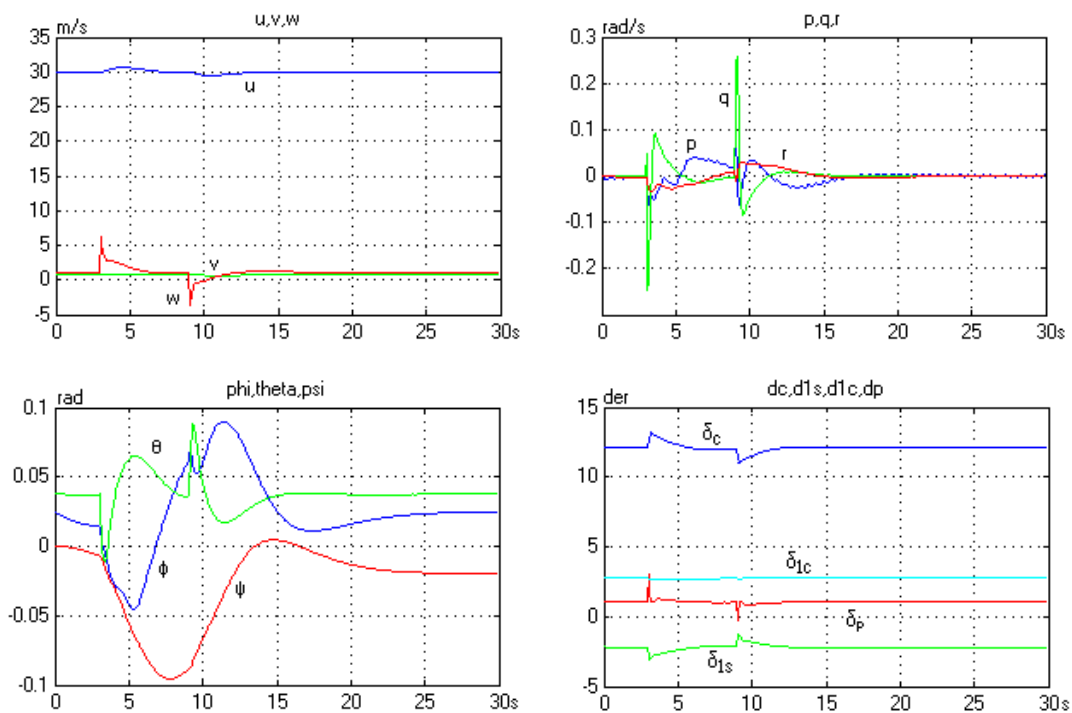


Figure 14 Rejection of vertical wind ( $h = 0\text{ft}$ ,  $u = 30\text{m/s}$ ): AFCS is on.

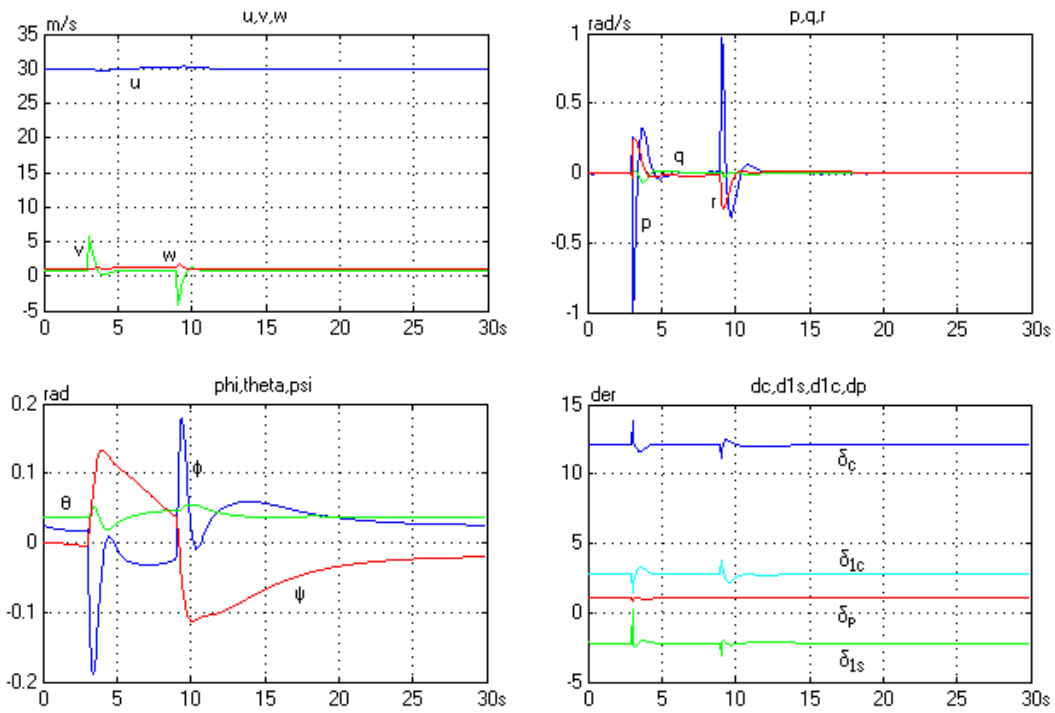


Figure 15 Rejection of side wind ( $h = 0ft, u = 30m/s$ ): AFCS is on.

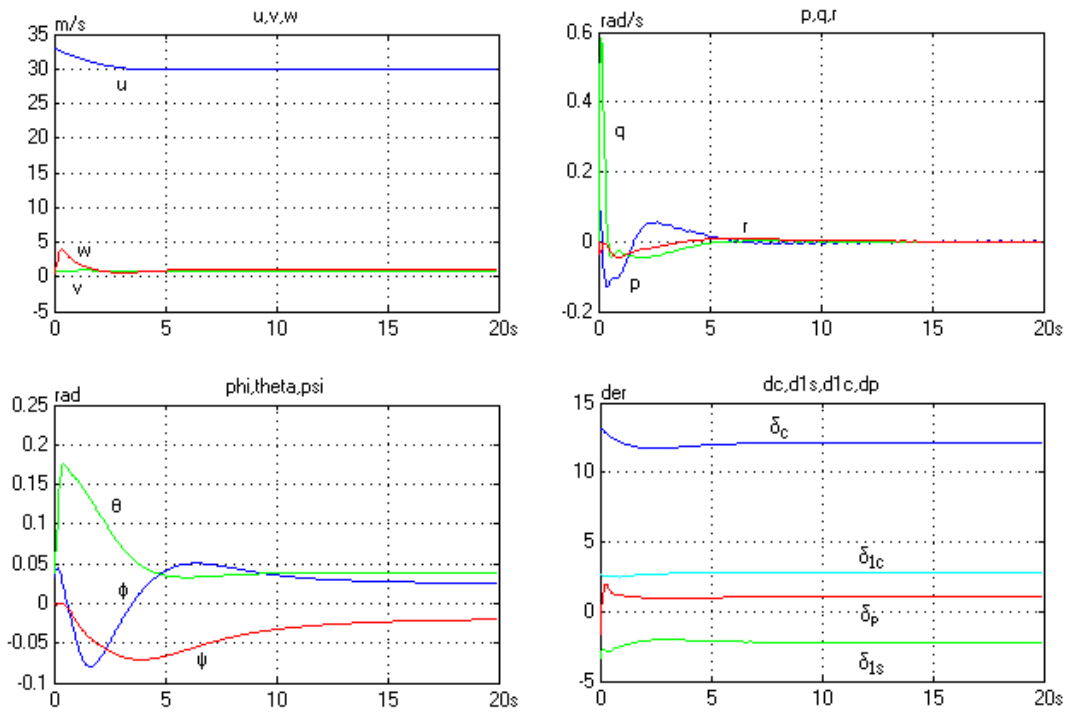


Figure 16 Forward speed correction manoeuvre ( $h = 0ft, u = 30m/s$ ): AFCS is on.

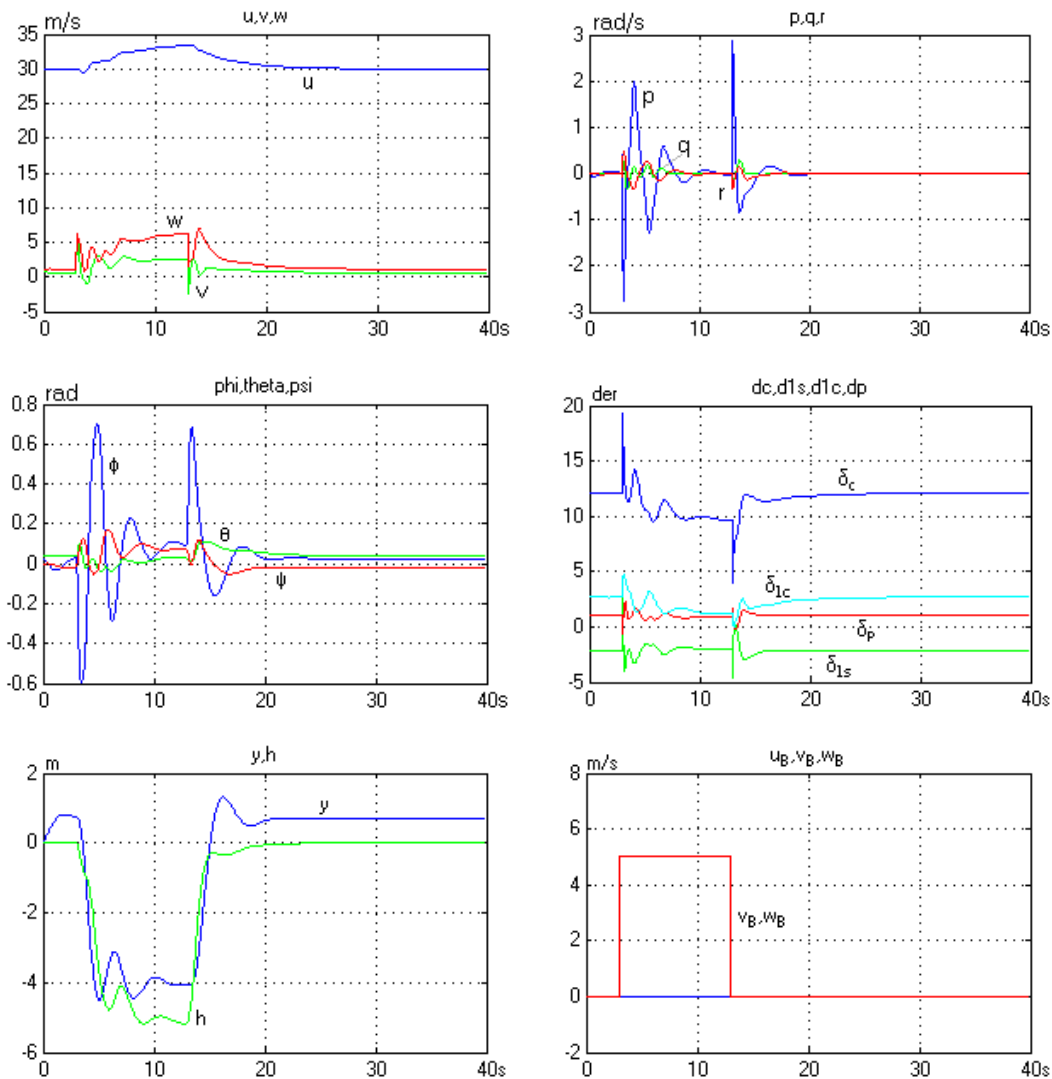


Figure 17 Rejection of vertical and side wind ( $h = 0\text{ft}$ ,  $u = 30\text{m/s}$ ): AFCS is on, speed hold is on, height hold is on, and heading hold is on.



Erkan Abdulhamitbilal was born in Balchik, Bulgaria in 1977. He received B.Sc., M.Sc., and Ph.D. degrees in Aeronautics and Astronautics Engineering from Istanbul Technical University (ITU), Turkey, in 2002, 2005, and

2010, respectively. He worked as a research engineer in stability and control group of Rotorcraft Research and Excellence Center of ITU under Project DPT-HAGU from 2003 to 2009. He is now with Altinay Robot Technologies and works as a research engineer in electrical car department, 2011. Dr. Abdulhamitbilal is the author of more than 20 international conference papers and research reports. His research interests include automatic control, variable structure control, flight dynamics and control, robot control.



Elbrous M. Jafarov was born in province Gokche (west Azerbaijan) in 1946. He received his M.Sc. degree in Automation and Control Engineering from Azerbaijan State Oil Academy (Baku) in 1969. The Ph.D. and D.Sc. (Eng) degrees

were received from NIPINefteKhimAutomat-TsNIIKAutomation (Moscow) and Institute of Cybernetics of Azerbaijan Science Academy; and Institute of Control Sciences (Moscow)-MIEM-LETI in Control Engineering in 1973 and 1982, respectively. He was the Head of Variable Structure Process Control Laboratory from 1969 to 1984, the Chairman of the Automation and Robotic Systems Department at the Az. TU during 1985-1996. He has been a professor in Istanbul Technical University since 1996. His research and teaching interests include control theory, sliding mode control, time-delay systems, robot control, robust control, optimal control.